



Downy mildew resistance is genetically mediated by prophylactic production of phenylpropanoids in hop

Alexander Feiner^{1,2}  | Nicholi Pitra³ | Paul Matthews³ | Klaus Pillen⁴ |
Ludger A. Wessjohann² | David Riewe^{5,6} 

¹Plant Science and Breeding, Simon H. Steiner, Hopfen GmbH, Mainburg, Germany

²Department of Bioorganic Chemistry, Leibniz Institute of Plant Biochemistry (IPB), Halle/Saale, Germany

³Research and Development, S.S. Steiner, Inc., New York

⁴Institute of Agricultural and Nutritional Sciences, Martin-Luther University (MLU), Halle/Saale, Germany

⁵Department of Molecular Genetics, Leibniz Institute of Plant Genetics and Crop Plant Research (IPK), Seeland, Germany

⁶Institute for Ecological Chemistry, Plant Analysis and Stored Product Protection, Julius Kühn-Institute (JKI), Federal Research Centre for Cultivated Plants, Berlin, Germany

Correspondence

Alexander Feiner, Plant Science and Breeding, Hopsteiner, Simon H. Steiner, Hopfen GmbH, Auhofstrasse 18, 84048 Mainburg, Germany. Email: alexander.feiner@hopsteiner.de

Funding information

Simon H. Steiner, Hopfen, GmbH

Abstract

Downy mildew in hop (*Humulus lupulus* L.) is caused by *Pseudoperonospora humuli* and generates significant losses in quality and yield. To identify the biochemical processes that confer natural downy mildew resistance (DMR), a metabolome- and genome-wide association study was performed. Inoculation of a high density genotyped F1 hop population (n = 192) with the obligate biotrophic oomycete *P. humuli* led to variation in both the levels of thousands of specialized metabolites and DMR. We observed that metabolites of almost all major phytochemical classes were induced 48 hr after inoculation. But only a small number of metabolites were found to be correlated with DMR and these were enriched with phenylpropanoids. These metabolites were also correlated with DMR when measured from the non-infected control set. A genome-wide association study revealed co-localization of the major DMR loci and the phenylpropanoid pathway markers indicating that the major contribution to resistance is mediated by these metabolites in a heritable manner. The application of three putative prophylactic phenylpropanoids led to a reduced degree of leaf infection in susceptible genotypes, confirming their protective activity either directly or as precursors of active compounds.

KEYWORDS

genome-wide association study, oomycete, untargeted metabolomics

1 | INTRODUCTION

Hop, *Humulus lupulus* L., is a dioecious perennial member of the *Cannabaceae* family (Neve, 1991). Its female flowers (cones) are mainly used in beer brewing as a flavouring as well as bittering agent because of the high abundance of secondary metabolites, including bitter acids, terpenes and polyphenols (De Keukeleire et al., 2003; Cleemput et al., 2009; Kavalier et al., 2011). In addition, numerous compounds make hops a source of pharmaceuticals in modern applications, with activity against metabolic syndromes (Cleemput et al., 2009; Miranda et al., 2018), anti-cancer (Farag & Wessjohann, 2013; Jiang, Sun, Xiang,

Wei, & Li, 2018; Krajnovic et al., 2019; Krajnovic, Kaluderovic, Wessjohann, Mijatovic, & Maksimovic-Ivanic, 2016) and phytoestrogenic properties (Possemiers et al., 2006; Stevens & Page, 2004; Wilhelm & Wessjohann, 2006). Diverse factors, such as a high degree of heterozygosity, dioecy and obligate outcrossing, a poorly understood gender-determination system and a large genome size of 2.7 Gbp (Padgitt-Cobb et al., 2019), contribute to the difficulty of hop breeding (Darby, 2006; Easterling et al., 2018; Neve, 1991; Zhang et al., 2017).

Pseudoperonospora humuli, the causal organism of hop downy mildew (DM), is an obligate biotrophic oomycete pathogen and has been a serious threat in recent years (Gent, Cohen, & Runge, 2017;

This is an open access article under the terms of the Creative Commons Attribution License, which permits use, distribution and reproduction in any medium, provided the original work is properly cited.

© 2020 The Authors. *Plant, Cell & Environment* published by John Wiley & Sons Ltd.

Neve, 1991). Especially in humid hop-growing areas, it is one of the most severe diseases that lead to losses in yield and quality, and current control of DM mainly depends on the use of pesticides or copper, as well as the planting of resistant genotypes.

Resistance to DM appears to be under quantitative genetic control in hop (Neve, 1991), and QTLs linked to DMR were identified with a high-density single nucleotide polymorphism (SNP) genetic map by Henning et al. (2015). Neither the infection process of *P. humuli* nor the underlying biochemical resistance mechanism against DM has yet been elucidated. However, the mechanism of resistance against DM infection in grapevine caused by *Plasmopara viticola* has been investigated using metabolomics, transcriptomics and proteomics (Ali et al., 2012; Batovska et al., 2009; Becker et al., 2013; Chitarrini et al., 2017; Legay et al., 2011; Milli et al., 2012). It has been reported that grapevine lacks a *P. viticola*-specific recognition system (Gasparo, Cipriani, Adam-Blondon, & Testolin, 2007) and that an activation of a successful inducible defence mechanism cannot occur (Legay et al., 2011; Ma et al., 2018; Perazzolli et al., 2012; Polesani et al., 2008; Su et al., 2018; Vannozzi, Dry, Fasoli, Zenoni, & Lucchin, 2012). According to Chitarrini et al. (2017), Nascimento et al. (2019) and Negrel et al. (2018), specified metabolites seem to be associated with the defence response.

Antimicrobial phenolic metabolites contribute to resistance against various pathogens (Chong, Poutaraud, & Huguene, 2009; Dixon, 2001; Dixon & Paiva, 1995) by inhibiting germination and growth as well as membrane permeabilization (Toffolatti, Venturini, Maffi, & Vercesi, 2012; Weidenbach et al., 2014). Such metabolites are also the precursors of lignin, which acts as a general barrier for pathogen progression into the cell wall (Vogt, 2010; Wang, Chantreau, Sibout, & Hawkins, 2013; Whetten & Sederoff, 1995). Studies on the role of phenylpropanoids in the defence response identified metabolites altered in response to infection with pathogens such as *Verticillium longisporum* (König et al., 2014), *Botrytis cinerea* or *Pseudomonas syringae* (Camañes, Scalschi, Vicedo, González-Bosch, & García-Agustín, 2015). In grapevine, infection with oomycetes led to an accumulation of stilbenes and specific gene expression responses in resistant genotypes (Figueiredo et al., 2012; Malacarne et al., 2011; Vannozzi et al., 2012).

In hop, chemical powdery mildew resistance markers have been investigated in the past (Cerenak, Kralj, & Javornik, 2009). By testing extremely susceptible and resistant cultivars, resistance-related metabolites (e.g., santalene, germacrene-D, or alpha-selinene) were identified because the elevation of their contents coincided inversely with the occurrence of powdery mildew infection. Thus far, untargeted metabolomics in hop has mainly been performed for the discrimination of cultivars (Farag, Mahrous, Lübken, Porzel, & Wessjohann, 2014; Farag, Porzel, Schmidt, & Wessjohann, 2012), genetic effects (Gatica-Arias et al., 2012), or medicinal properties (Farag, Weigend, Luebert, Brokamp, & Wessjohann, 2013), but has not been applied for the elucidation of biochemical resistance mechanisms against diseases such as DM.

The primary objective of this research was the integration of metabolomic, phenotypic and genetic information to understand

pathogen response on a biochemical and molecular level. The identification of SNP markers and secondary metabolites associated with (and predictive for) DMR contributes to an increase in the knowledge of disease resistance mechanisms. Our results show that DMR in hop is primarily conferred by at least two loci regulating the abundance of phenylpropanoids among 192 siblings in a hop bi-parental mapping family. The protective activity of phenylpropanoids against DMR was further confirmed in a bioassay. A global analysis of metabolite-DMR correlations between a non-infected and an infected set revealed that resistance is established per se, prior to infection with the pathogen.

2 | MATERIAL AND METHODS

2.1 | Mapping population

A mapping population was produced by crossing the DM-resistant line “Yeoman” (female, Neve, 1991) with the DM-susceptible line “USDA21588m” (male, USDA, 2018). The parents were grown in 2014 for 150 days in an experimental nursery in Yakima, WA, USA, until flowering occurred, and pollination was conducted by cross-pollination. After 60 days, seeds were collected.

After stratification for 6 weeks at 4°C, seeds were germinated in moist Jiffy pots (Jiffy, 44 mm) and grown in an incubator (DR-66VL, CLF PERCIVAL). One hundred and ninety-two F1 genotypes (males and females, undetermined) were randomly selected. The plants were cultivated at 130 µmol/m²/s, 18°C during the day (16 hr) and 16°C at night (8 hr) with a relative humidity of 75%.

2.2 | Cloning and fertilization of seedlings

Seedlings were cloned 7 weeks after germination. Sterile softwood wedges (102 cell counts per tray, Oasis) were used for propagation into two identical sets, one for infection and one for mock treatment. After 4 weeks, cuttings were repotted into 5 × 5-cm pots using sterilized and steamed potting soil. To stimulate axillary meristem growth and root development apical growth, tips were pinched aseptically after two sets of leaves were developed. Plants were fertilized by applying 500 ml N/P/K- ratio of 8/8/6 in a 0.2% concentration (Kamasol brilliant blau) directly into each tray 20 and 35 days after cloning.

2.3 | Isolation and infection with *Pseudoperonospora humuli*

An aggressive *P. humuli* isolate from Wye Hops, Ltd, U.K. was selected and cultivated using the susceptible cultivar “Hallertauer Mittelfrüh” (Biendl et al., 2014) as host. Seven weeks after cloning, when the majority of plants were in the BBCH 19 stage (Rossbauer, 1995), inoculation with *P. humuli* was applied. Incubator conditions were set to 16°C day (16 hr) and 15°C night (8 hr) temperature during the

infection with 99% relative humidity to create ideal infection conditions (Mitchell, Ocamb, Grunwald, Mancino, & Gent, 2011; Neve, 1991; Royle & Thomas, 1973). The sporangia were washed from infected host leaves with 4°C cold deionized H₂O. The abaxial leaf surfaces were inoculated with a suspension of *P. humuli* (ca. 1×10^5 sporangia/ml, adjusted with Neubauer hemocytometer) using a hand-held atomizer (reagent sprayer, CAMAG) until the whole leaf surface was covered with fine droplets. After inoculation, plants were covered for 24 hr in darkness with lids to keep humidity as high as possible (Cohen & Eyal, 1980; Johnson & Skotland, 1985; Mitchell et al., 2011; Royle & Thomas, 1971, 1973). Mock infection with deionized H₂O was applied to a replicate plant set including all 192 genotypes. Five days post-infection, the conditions were returned to 18°C during the day (16 hr)/16°C during the night (8 hr), and plants were covered with lids again inducing high humidity to optimize the secondary infection event (Mitchell et al., 2011).

2.4 | Disease scoring

Seven days post infection, visual disease scoring of the infected set was performed three times in a random order in two independent experiments. Five categories (Bundessortenamt, 2000) were used to score the DM infection (1 = highly tolerant, no sporulation; 3 = tolerant, 1–20% of leaf area infected; 5 = medium infected, 21–50% leaf area infected; 7 = susceptible, 51–80% leaf area infected; 9 = highly susceptible, 81–100% leaf area infected). Due to safety and quarantine rules, both parents (Yeoman, USDA21588m) could not be grown in the S1 area at the Leibniz-Institute for Plant Biochemistry (IPB). Therefore, their disease score under phyto chamber conditions was calculated by interpolating the disease score of the mapping population and both parents under field conditions.

2.5 | Leaf sampling

Within 2 hr in the middle of the light period, three fully developed leaves per individual were frozen in liquid nitrogen 48 hr after inoculation. The samples were stored at –80°C until extraction.

2.6 | Extraction of specialized metabolites

Deep-frozen sample material was re-randomized and homogenized using a robotic cryogrinder (Cryo Grinder, Labman Automation Ltd.) as described previously (Wiebach, Nagel, Börner, Altmann, & Riewe, 2019). 150 ± 10 mg fresh weight leaves was extracted with 1.5 mL of methanol by shaking for 15 min followed by 15 min of ultrasonification at 4°C (Riewe et al., 2012, 2016). After 15 min of centrifugation at 20,800 rpm at 4°C (Eppendorf Centrifuge 5417R, Eppendorf AG), 300 µl of the supernatant was aliquoted into LC–MS vials (CZT Trott) and dried for 3 hr at 10 mbar in a speedvac (RVC 2-33, Martin Christ GmbH). The dried vials were filled with argon and stored at –80°C until LC–MS analysis.

2.7 | High-resolution liquid chromatography-mass spectrometry (LC–MS) analysis

Randomized samples were re-solubilized in a maximum of 500 µl 100% methanol. Twenty-four hours prior to injection, 1.2 µl of extract were injected using an MPS2 autosampler (Gerstel). Analytes were separated by UHPLC (1290 UHPLC, Agilent) using a C18-column at 50°C (50 mm length \times 1 mm i.d., 1.8 µm particle o.d., Waters) with mobile phases of 0.1% formic acid in water (A), and 0.1% formic acid in acetonitrile (B). The gradient was 0.5 min: 1% B, 1.75 min: 30% B, 2.25 min: 60% B, 3.75 min: 90% B, 4 min: 99% B, 4.5 min: 99% B, 4.75 min: 1% B, 5 min: 1% B. The flow rate was 800 µl/min. MS spectra were recorded with a Bruker Maxis HD mass spectrometer upgraded with a Maxis II detector (Bruker) at a frequency of 5 Hz from 100 to 1,500 m/z, dry temperature: 250°C, capillary voltage: 4500/–3,000 (positive/negative mode), nebulizer pressure: 4 bar, dry gas: 12 L/min, dry temperature: 250°C. Data were externally and internally calibrated and exported as a net.CDF file as described previously by Riewe, Wiebach, and Altmann (2017). MS/MS spectra were collected from a pooled sample in auto-MS/MS mode using a scheduled precursor list (SPL). Of all potentially monoisotopic peaks from the profiling experiment, retention time (± 1 s) and m/z (± 20 mD) was extracted to create the SPL in a format applicable to the mass spectrometer. If an m/z of a precursor scan matched to a feature in the SPL, an MS/MS spectrum was recorded during the following scan.

2.8 | Raw data processing

LC–MS chromatograms in net.CDF format were processed using “xcms” (Smith, Want, O’Maille, Abagyan, & Siuzdak, 2006; Kuhl, Tautenhahn, Boettcher, Larson, & Neumann, 2012) and “CAMERA” as described previously by Riewe et al. (2017). The initial peak tables had 37,386/20,899 (positive/negative mode) peaks. Peaks eluting between 4 and 270 s after injection and peaks found in more than two blank extracts with a median higher than half of the sample median (background) were discarded. All m/z were modelled using annotation errors as described previously to increase mass accuracy. Peak areas were normalized to fresh weight and median value per metabolite for each of the four extraction batches. MS/MS spectra were processed exactly as described above.

2.9 | Peak annotation and representation analysis

All m/z were queried against the Kyoto Encyclopedia of Genes and Genomes (KEGG) database (Release 86.0, Kanehisa & Goto, 2000) as [M+H]⁺ and adducts, including [M+Na]⁺, [M+CH₃OH+H]⁺ (positive mode), [M–H][–], [M–H₂O–H][–] or [M+FA–H][–] (negative mode), using KEGGREST (Tenenbaum, 2018). Sum formulae, KEGG-IDs, names, reactions, pathways and BRITE annotations were retrieved for each identified m/z.

For validation of the peak annotation process, 45 reference compounds known to be present in hop were used as authentic standard

(Table S1). In addition, MS/MS spectra of reference compounds and all detected metabolites in the pool sample were considered for the validation of the peak annotation.

2.10 | DM protection assay

Ten DM susceptible genotypes (ID 27, 31, 34, 43, 45, 46, 101, 148, 156, 168, Table S2) were cloned and cultivated as described above to produce asymptomatic test plants.

Fifty days after propagation, the abaxial leaf area of three replicates of each genotype were sprayed using a hand-held atomizer (CAMAG, reagent sprayer) until the whole leaf was covered with fine droplets. Either protection (1 mM chlorogenic acid, *p*-coumaric acid and coniferyl aldehyde, Sigma Aldrich) or mock solution (H₂O) was applied, and 2 hr later they were sprayed with a *P. humuli* suspension (1×10^5 sporangia/ml, adjusted with Neubauer haemocytometer) or mock control (H₂O) in 2×2 factorial design. An average of 3 ml of the solution was sprayed onto the leaf surface. The average weight of the leaf mass of a plant was 3 g, therefore, it can be assumed that a 1:1 application (volume spray: weight of leaf material) was executed.

Seven days later, the plants were disease phenotyped as indicated above.

2.11 | DNA extraction

Approximately 50 mg leaf material was lyophilized and sent to LGC Genomics (Berlin, Germany) for further analysis. Total genomic DNA for library construction and sequencing was isolated using the extraction method published by Xin and Chen (2012) with a subsequent normalization step.

2.12 | Normalized genotyping by sequencing (nGBS) using *Msi*I

Normalized Genotyping by Sequencing (nGBS) using *Msi*I, data analysis and read pre-processing was executed using the protocol applied in Maghuly, Pabinger, Krainer, and Laimer (2018). LGC provided quality trimmed 150 bp PE reads and quality trimming of adapter clipped Illumina reads was executed according to Maghuly et al. (2018).

2.13 | GBS alignment and SNP discovery

Reads were aligned to the Cascade hop reference genome (Padgitt-Cobb et al., 2019) using the Burrows-Wheeler Alignment tool (BWA; Li & Durbin, 2009). The pipeline for creating a variant call format (vcf) file was run with samtools and bcftools mpileup according to the workflow provided on the Samtools website "http://www.htslib.org/workflow" (Li et al., 2009).

2.14 | SNP filtering and linkage grouping

SNPs with distorted segregation patterns were filtered out using Rqtl (Broman, Wu, Sen, & Churchill, 2003). Markers of the F1 population with heterozygosity only present in the maternal genotype (crossing scheme: Aa \times AA) with minor allele frequencies (MAF) > 0.1 and no missing data were selected. Markers containing single alleles with unpredicted allele states among less than 5% of individuals were nevertheless kept in the study, but the allele was set to missing data. A maternal linkage map was constructed using the backcross (BC1) population type in JoinMap (Van Ooijen, 2011). Markers were placed into linkage groups (LG) using default settings in JoinMap and a LOD value cut-off greater than 4.0. Applying the strongest cross-link (SCL) parameter supported the identification of proper LG assignments. Ungrouped markers were combined into an additional LG (LG0). Cut-off number of SNPs to form an LG were set to >5 SNPs. Unpredictable translocation events segregation distortion in hop (Easterling et al., 2018; Zhang et al., 2017) does not allow a precise ordering of markers within linkage groups. Therefore, markers within LGs were arranged in ascending order according to their DMR association p-value. This linkage grouping was used to display the coincidence of DMR and metabolite associated markers within the established linkage groups.

2.15 | Sequence analysis using BLAST

DNA sequences were aligned to the Cascade hop reference genome (Padgitt-Cobb et al., 2019) to construct contiguous scaffolds. Hotspots (100 kb) on scaffolds containing SNPs significantly associated with DMR were aligned to the plant unigene database at NCBI (NCBI, 2018) using BLAST (Basic Local Alignment Search Tool; Altschul, Gish, Miller, Myers, & Lipman, 1990). The molecular function of all homologs was manually inspected in the source organism *Arabidopsis thaliana* to assess the candidate's potential involvement in resistance to pathogens using "The Arabidopsis Information Resource" (TAIR, release version 10, Lamesch et al., 2012).

2.16 | Statistical analysis

Metabolite data were \log_{10} -transformed for ANOVA testing and Box-Cox-transformed (Box & Cox, 1964) for Pearson correlation testing using R (R Core Team, 2018). Representation analysis of induction/reduction of metabolites within KEGG BRITE classes was executed using binomial testing as conducted previously (Wiebach et al., 2019). False discovery rate corrections were applied as described by Benjamini and Hochberg (1995). A *t*-test was applied for the DMR protection assay. Overlap of DMR and phenylpropanoids was determined using a χ^2 -test.

To investigate marker-trait association, the general linear model (GLM) in TASSEL using default settings (Bradbury et al., 2007) was applied. False discovery rate (FDR) corrections were applied as

described by Benjamini and Hochberg (1995). A χ^2 test was executed to test the association marker overlap of DMR and significantly DMR-correlated compounds in both treatments, infected and mock.

2.17 | Data deposition

Supporting Information Tables S3 and S4 are available from RADAR (www.radar-service.eu) and can be accessed at <https://dx.doi.org/10.22000/319>.

3 | RESULTS

3.1 | Generation of a hop F1 mapping population with genetic variation in DMR

192 F1 genotypes were produced from the cultivar “Yeoman” (resistant, female) and the wild-type “USDA21588m” (susceptible, male) by cross-pollination. In two independent experiments, replicated and synchronized clones were grown for 7 weeks in an incubator. After this period, one replicated set was inoculated with *P. humuli*, and another set was mock-inoculated with deionized H₂O. After 7 days, the inoculated set was phenotyped with respect to the degree of DM infection (Figure S1) and displayed normally distributed large variation in the DMR scores (Figure S2 and Table S2). There was no significant difference between the two replications according to ANOVA ($p = 0.27$). Broad-sense heritability was relatively high ($h^2 = 0.81$), indicating that genetic control over DMR is high and environmental influences within the experiment were low. It was not possible to include the F1 parents due to safety regulations, but based on field data, we can estimate that “Yeoman” would have a DMR score of 2.2 and “USDA21588m” a DMR score of 8.3 in this study (see material and methods for more details).

3.2 | Untargeted profiling and annotation of specialized metabolites

Leaf samples were taken from the infected and control set 2 days after inoculation with *P. humuli*. Polar metabolites from all 384 samples were extracted and analysed using LC-MS in both positive and negative mode. Per extract, 27,324 (positive mode, Table 1 and Table S3) and 16,256 (negative mode, Table 1 and Table S4) redundant chromatographic mass-to-charge (m/z) features were recorded and remained after background subtraction, forming 10,781 (positive) and 7,361 (negative) non-redundant pseudospectra with base peaks likely representing individual metabolites (Kuhl et al., 2012). All m/z were queried against compounds in the Kyoto Encyclopedia of Genes and Genomes database (Kanehisa & Goto, 2000) with an error tolerance of 0.5 ppm, but only annotations of monoisotopic base peaks with an isotope pattern fit of <60 mSigma (Thiele, Mcleod, Niemitz, & Kühn, 2011) are discussed below (Tables S3, S4 “Annotation filter”).

One or more KEGG sum formulae/structures were assigned to 512 (positive) and 666 (negative) base peak m/z , and 259 (positive) and 395 (negative) of these base peaks received a “phytochemical compound” annotation. Table 1 lists the number of “phytochemical compounds” tentatively detected two levels down the KEGG BRITE compound-specific hierarchical relationships. While the detected number of compounds relating to alkaloids, fatty acids and amino acids data were low in both modes (< 15 per class), the number of flavonoids, phenylpropanoids and terpenoids was relatively high (> 60). In general, there was consistency in the number of detected metabolites per class between positive and negative mode.

3.3 | DM infection triggers a large mobilization of specialized metabolites

Although no visible phenotypic differences between the infected and control plants were observed 48 hr after infection, this time point was chosen because the earliest metabolic changes were detectable then in preceding studies on grapevine (Chitarrini et al., 2017; Toffolatti et al., 2012). To test if a biochemical defence response 48 hr after infection was present, we compared the level of salicylic acid as a common metabolite related with defence response (validated by an authentic standard, Table S1) between the infected and the mock set. On average, the 192 infected plants contained 2.1 times more salicylic acid than their 192 mock controls (false discovery rate [FDR] = 5.8×10^{-34}). From this relatively high degree of induction within the dataset (see below and Figure 1a,b), we conclude that early molecular defence processes are active and detectable at this time point after infection. Subsequently, we tested all non-redundant features for differential abundance using ANOVA. We found that the levels of 3,358 out of 10,781 (31%, positive) and 2,109 out of 7,361 (29%, negative) base peaks were significantly altered between the infection and control set (Table 1 and Figure 1a,b). Of these, 2,825 (84%, positive) and 1,853 (88%, negative) base peaks were more abundant in the infection set. This clear trend towards production of metabolites in response to infection is even more evident for the base peaks with phytochemical annotation. One hundred and fifty-one (58%, positive) and 185 (46%, negative) of these metabolites were altered (Table 1 and Figure 1c,d) and out of these, 143 (95%, both modes) and 179 (97%, negative) were more abundant in the infection set. The production of specialized metabolites was also found to be significant for all compound classes that could be tested using an FDR-corrected binomial test (>7 up- or down-regulations). Roughly one third of all compound classes, typically the more abundant classes mentioned above, showed significantly more metabolite inductions than reductions in both detection modes. Apart from the 20/10 (positive/negative) carotenoids and apocarotenoids, of which 4/2 (positive/negative) were found to be reduced upon infection, there was not a single phytochemical class with significantly more compound reductions than elevations in the KEGG BRITE system. Notably, six compounds with KEGG annotation of either coumaroyl-putrescine or feruloyl-putrescine were found among the 25 most reduced base peaks in positive ion mode. Though known plant metabolites, these

TABLE 1 MS processing

Feature type/annotation	Positive mode Up/down/total	Negative mode Up/down/total
m/z (after background subtraction)	8971/1330/27324***	4165/505/16256***
Pseudospectra/base peaks	2825/533/10781***	1853/256/7361***
Base peaks with KEGG annotations	265/20/512***	286/11/666***
KEGG BRITE phytochemical annotations	143/8/259***	179/6/395***
Alkaloids	4/2/12	4/1/5
Derived from ornithine	0/0/1	0
Derived from lysine	0/0/2	0/1/1
Derived from nicotinic acid	0	1/0/1
Derived from tyrosine	3/0/3	2/0/2
Derived from tryptophan and anthranilic acid	3/2/8	3/1/4
Derived from histidine	0	0
Derived by amination reactions	0	0
Others	0	0
Flavonoids	42/0/75***	44/0/103***
Flavonoids	34/0/63***	34/0/82***
Isoflavonoids	16/0/23**	26/0/45***
Complex flavonoids	6/0/10	3/0/12
Phenylpropanoids	30/1/61***	37/1/91***
Monolignols	4/1/18	9/0/37*
Lignans	17/0/21**	24/0/40***
Coumarins	10/0/27*	19/1/38**
Shikimate/acetate-malonate derived	16/0/22**	8/0/16*
Stilbenoids	12/0/17*	4/0/12
Others	4/0/5	4/0/4
Terpenoids	81/5/132***	127/4/255***
Hemiterpenoids (C5)	0	0
Monoterpenoids (C10)	13/1/19*	22/0/54***
Sesquiterpenoids (C15)	29/0/43***	57/0/108***
Diterpenoids (C20)	42/0/58***	65/0/106***
Sesterterpenoids (C25)	0	0
Triterpenoids (C30)	15/0/28**	50/1/79***
Steroids	6/0/8	23/1/39***
Carotenoids and apocarotenoids	6/4/20	2/2/10
Others	0	0
Polyketides	22/1/37**	36/1/69***
Anthraquinones	8/0/11*	5/0/12
Pyrones	4/0/15	11/1/25*
Others	10/1/12*	21/0/34***
Fatty acids related compounds	0/0/4	5/0/11
Fatty acids	0/0/4	5/0/11
Amino acid related compounds	1/0/3	1/0/2
Betalains	0/0/1	0
Cyanogenic glucosides	1/0/1	0
Glucosinolates	0	0
Others	0/0/1	1/0/2

TABLE 1 (Continued)

Feature type/annotation	Positive mode Up/down/total	Negative mode Up/down/total
Others	3/0/5	4/0/8
Naphthoquinones	0/0/2	1/0/2
Tannins and galloyl derivatives	0	0
Others	3/0/3	3/0/6
	Correlated/total	Correlated/total
Pseudospectra/base peaks	177/10781	118/7361
Phenylpropanoids	4/61*	8/91***
Coumarins	3/27*	6/38***
Monolignols	3/18**	6/37***

Note: Differentially abundant features/annotations 48 hr after inoculation with *Pseudoperonospora humuli* and correlated to disease score 7 days after inoculation.

*FDR-P < 0.05.

**FDR-P < 0.005.

***FDR-P < 0.0005.

compounds do not yet have a KEGG BRITE annotation; they are amides of phenylpropanoids and the polyamine putrescine. While the fraction of significantly elevated phytochemical compounds is relatively high, the magnitude of their accumulation is moderate. With very few exceptions, the increase in abundance of elevated phytochemicals was between 5 and 60% in both modes (Figure 1a–d) and reductions were of lower magnitude. In conclusion, *P. humuli* elicits a broad but unspecific production of specialized metabolites in the hop leaf within 48 hr.

3.4 | DMR is correlated with a small set of metabolites with putative protective function

It appeared unlikely that all the (polar) metabolites found to be differentially abundant in this untargeted study were involved in a stress response role. We thus searched for metabolites protective against DM in a dose-dependent manner by calculating Pearson correlations between DMR scores 7 days after inoculation with *P. humuli* and each metabolite level in this set, sampled 5 days earlier, at 48 hr after inoculation. To account for the differences in sampling time when connecting two different data domains and the unavoidable inaccuracies connected with visual and categorical scoring of DMR, we raised the FDR to 0.1. However, only 166 out of 10,781 (positive) and 55 out of 7,361 (negative) metabolites displayed significant correlations (FDR < 0.1) to DMR within the infected set, with R ranging between –0.38 and 0.33 and a normal distribution centered around 0 (Figure 1g,h, X-axis). Figure 1e shows the second strongest out of 10,781 correlations between a base peak (R = 0.34, ID = p6197 in Table S3) from the infected sample set to the DMR score. The disease score is lower when the metabolite is more abundant, providing evidence for a putative protective function of this metabolite against DMR. One hundred and thirty-four (positive) and 12 (negative) base peaks were negatively correlated with the disease score. These correlations are in support of the hypothesis that the

resistance of hop against DM is, at least in part, executed by small molecules with protective properties.

3.5 | DMR is predictable from uninfected control samples

Analogous to the correlations calculated above within the infected set, we also determined the correlations between DMR arising from the infected plant set to the metabolite levels of the mock-infected plant set 48 hr after mock inoculation. Unexpectedly, here too a comparable number of metabolites correlated with DMR (28 positive, 82 negative, FDR < 0.1, Tables S3, S4) were identified, and the range of R was similar (–0.37 to 0.31, Figure 1g,h, Y-axis). Figure 1f again shows the correlation between ID p6197, this time determined in the mock-treated samples, to DMR in the infected sample set. It is the highest correlated metabolite out of 10,781 with the same degree of correlation as found within the infected set (R = 0.34). The possibility that these correlations were caused by a response of the control plants to contamination with *P. humuli* can be excluded because they showed no signs of DMR 7 days after mock inoculation. These results provide evidence that DMR is dependent on the heritable metabolic status in the hop leaf before or at the time of pathogen attack.

3.6 | DMR is pre-established in hop

Motivated by the finding that p6197 exhibited the second highest correlation with DMR out of 10,781 values when measured in the infected set, and the highest when measured in the control set, we searched for such co-incidences systematically. By comparing the correlation coefficients of the infected (R_{infected}) with the control set (R_{Mock}), we found that there was an overall relationship between the putative protective metabolites detected by correlation analysis from the infected set and

those found to be predictive from the analysis of the control set. As described above for p6197, many other base peaks found to be predictive in the mock control set were also protective at a comparable level in the infected set. There was a highly significant correlation between R_{Infected} and R_{Mock} independent of whether we tested metabolites collected in positive ($R = 0.53$, $p < 2.2 \times 10^{-16}$) or negative mode ($R = 0.54$,

$p < 2.2 \times 10^{-16}$, Figure 1g,h). Therefore, we conclude that protective metabolites are pre-formed before *P. humuli* is inoculated, and to a large degree are responsible for DMR. This also applies in particular to metabolites with high potential protective activity considering their individual bioactivity profiles as known from literature (Chong et al., 2009; Dixon, 2001; Dixon & Paiva, 1995).

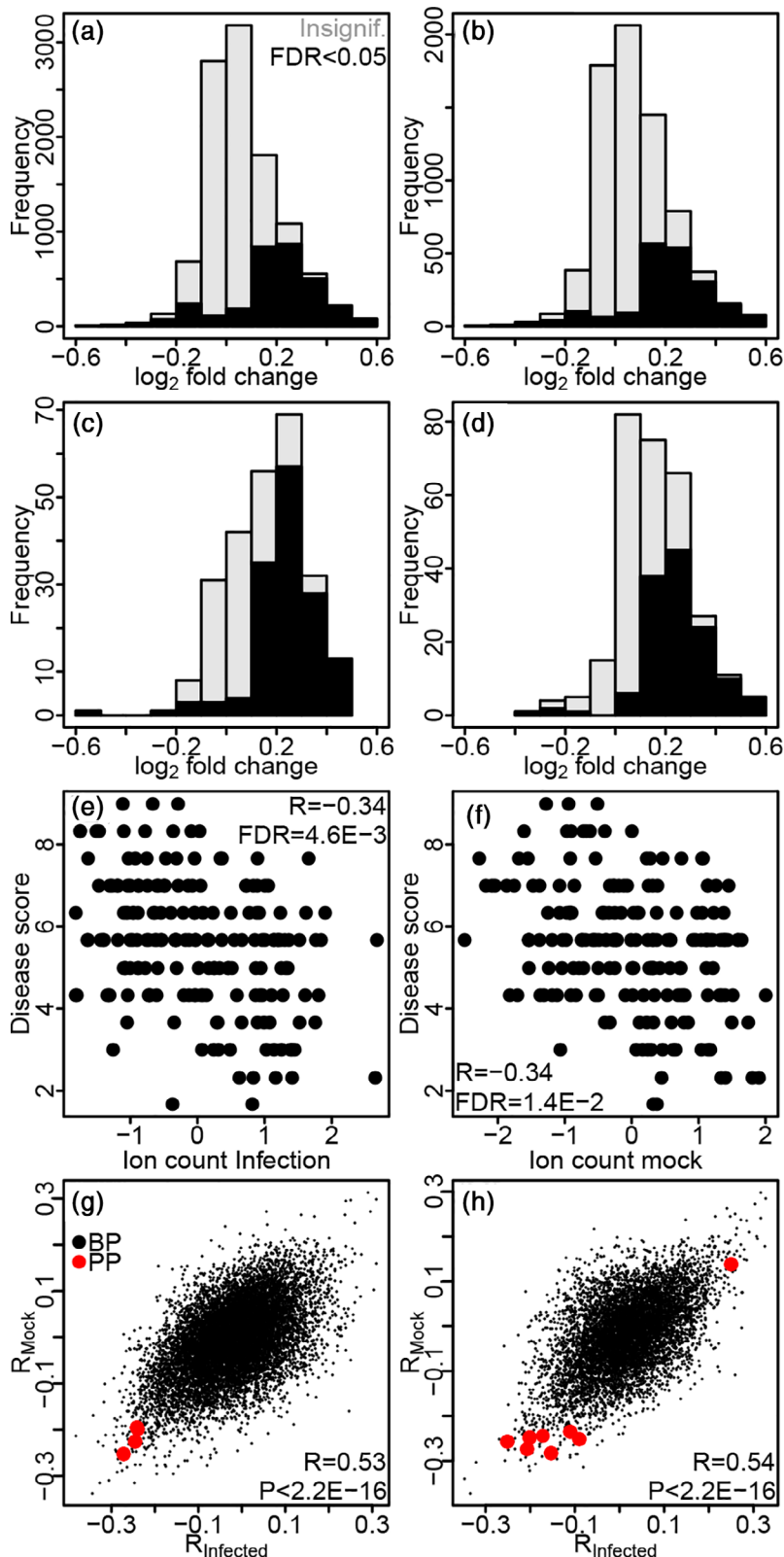


FIGURE 1 *Pseudoperonospora humuli*-induced phytochemical response in the hop leaf, metabolite-to-DMR correlations and DMR protection assay. \log_2 -fold changes of metabolites quantified in (a) positive and (b) negative mode 48 hr after infection. \log_2 -fold changes of metabolites with phytochemical annotation in (c) positive and (d) negative mode. Correlation between DMR 7 days after infection and the power-transformed, scaled and centered ion count of ID p6197, quantified in leaves 48 hr after infection from the (e) infected plant set and the (f) mock treated plant set. Correlation between the DMR-to-metabolite correlation coefficients from the infected plant set (R_{Infected}) and the DMR-to-metabolite correlation coefficients from the mock treated plant set (R_{Mock}) in (g) positive and (h) negative mode; small black points = base peaks, large red points = DMR-correlated phenylpropanoids. $n = 188/189$ for infected/mock in (a) and (c), $192/192$ for infected/mock in (b) and (d), 188 (e), 189 (f), $10,781$ (g) and $7,361$ (h)

3.7 | Phenylpropanoids have the highest DM-protective potential

An ANOVA led to no conclusive results with respect to compound classes involved in DMR because metabolites of virtually all phytochemical classes were induced 48 hr after infection. We then searched for compound classes with significantly enriched metabolites correlated to DMR. According to dose–response relationships, such metabolites might possess direct biological activity against the pathogen or its infection mechanism. All annotations belonging to the KEGG BRITE classes two hierarchy levels downstream of “phytochemical compounds” were tested for overrepresentation using a chi-square test. The sum of correlated base peaks (FDR < 0.1) determined in both infected and mock sets divided by the total number of base peaks was used as probability. Strikingly, only phenylpropanoids and the related coumarin and monolignol subclasses were significantly more often correlated with DMR than would be expected (Table 1, bottom). As shown in Figure 1g,h and in support of their putative beneficial role in DMR, these phenylpropanoids were almost exclusively negatively correlated with the DM disease score (Figure S3 for phenylpropanoid levels in all genotypes). The availability, or even direct biological activity, of phenylpropanoids plays a more relevant role in DMR than other phytochemical compounds within the KEGG BRITE classification system.

3.8 | Application of a phenylpropanoid-cocktail protects hop from DM

Two of the most highly correlated phenylpropanoids were tested for their protective activity against DM. Chlorogenic acid (positive mode: p10896, p10893; negative mode: n4563, n4564) and coniferyl aldehyde (positive mode: p3313) were the chosen candidates and inoculated alongside with *P. humuli*. In addition, *p*-coumaric acid was chosen as a third candidate, as it also strongly correlated with DMR (positive mode: p2542, negative mode: n554, Table S3, S4). According

to the peak intensity of an authentic standard, the median endogenous foliar concentration of *p*-coumaric acid is approximately 50 μ M, ranging from 10–100 μ M. Due to the labor-intensiveness associated with protection testing, all three compounds were tested in combination at a concentration of 1 mM each. They were sprayed 1:1 (spray volume:plant leaf weight). This would lead to a maximal increase of the endogenous concentration in the range of one to two orders in the case all *p*-coumaric acid would have been incorporated.

The infection and phenotyping of DM infection were assessed using categories (1 = resistant, 9 = highly susceptible) as outlined in the inoculation test. While sole application of the phenylpropanoid mix (Pro/Moc, Figure 2c,e) led to no detectable effects compared to control plants (Moc/Moc, Figure 2d,e), infection with *P. humuli* (Moc/Inf) led to the expected development of DM.

In contrast, however, co-inoculation of *P. humuli* and the phenylpropanoid mix (Pro/Inf) resulted in reduced leaf infection when compared to infected plants not treated with the phenylpropanoids (Moc/Inf, $p = 5.2 \times 10^{-4}$), thus providing further independent evidence for their protective activity in combination – not excluding that a single component may be responsible for most of the effect.

3.9 | DMR is controlled by two major loci

The development of the genetic map requires a complete whole-genome chromosome assembly, which is currently not available for hop. In addition, most existing algorithms used in genetic mapping were designed for inbred lines (e.g., *Arabidopsis*) but are not particularly suitable for hop with its heterozygous and extremely complex genome (Zhang et al., 2017). Therefore, a linkage grouping without ordering markers was preferred in this study over a genetic map with a high probability of incorrect ordering.

A linkage grouping using SNP markers was created using JoinMap. Prior to calculation, SNP marker filtering was applied to eliminate markers with distorted segregation and non-Mendelian segregation. Two thousand and fifty non-redundant markers with a minor allele

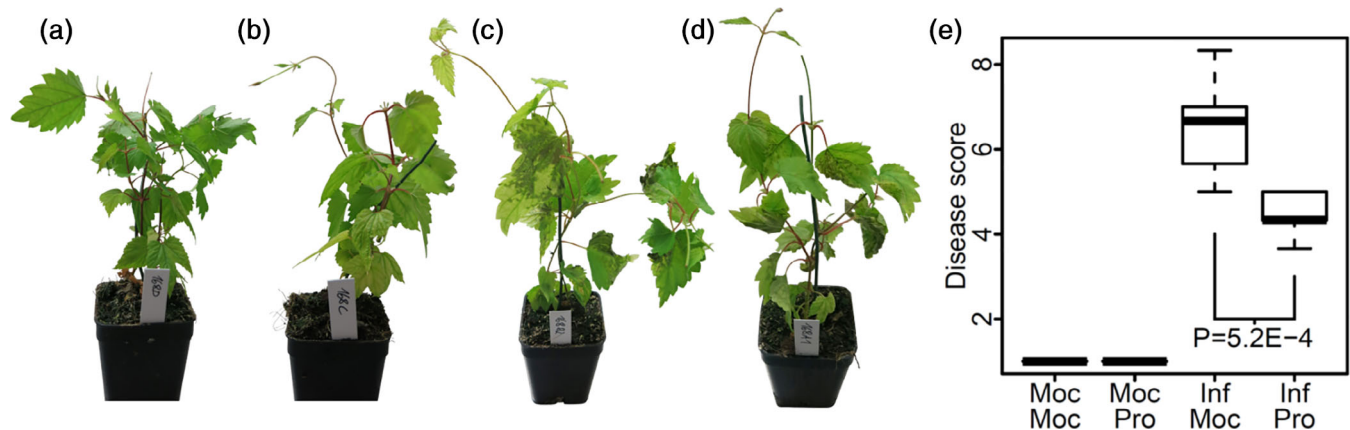


FIGURE 2 Phenotypic effects of the four conditions in the DM protection assay on genotype 168. (a) Moc/Moc. (b) Moc/Pro. (c) Inf/Moc. (d) Inf/Pro. Pot size = 5 × 5 cm. (e) Candidate metabolites protection assay, Moc = H₂O control for either protection or infection solution/suspension, Pro = protection solution with 1 mM candidate metabolites, Inf = infection suspension with *P. humuli*. $n = 10$

frequency (MAF) between 0.20 and 0.35 (Figure S4) on 175 scaffolds were left for grouping within the maternal segregation type. After filtering of SNPs, the linkage grouping was calculated. In the maternal grouping, 1,581 markers could be grouped within 16 linkage groups (LGs). Four hundred and seventy markers remained ungrouped and were assigned to one additional LG (LG 0). The distribution of markers across LGs was unbalanced. The number of markers in the grouping varied from a high number of 860 in LG 1 to six markers in LGs 11, 15 and 16.

All 2,050 markers were retained, and the general linear model (GLM) was used to assess DMR genotype–phenotype associations. Four hundred and twenty significant markers ($FDR < 0.05$) grouped to LG 1 and 246 ungrouped markers (LG 0) showed a significant association to DMR across the mapping population (Figure 3, Table S5).

3.10 | Genetic DMR and phenylpropanoid markers overlap

Metabolite-marker associations were calculated for the 12 phenylpropanoids as described for DMR, and the significance of the overlap between Phenylpropanoid and DMR marker was determined using a χ^2 test (Table 2). Three out of 12 compounds revealed a significant overlap with DMR association in both treatments. These are Fraxin (n5122), 4-coumaryl alcohol/5-hydroxyconiferyl alcohol (n1121) and

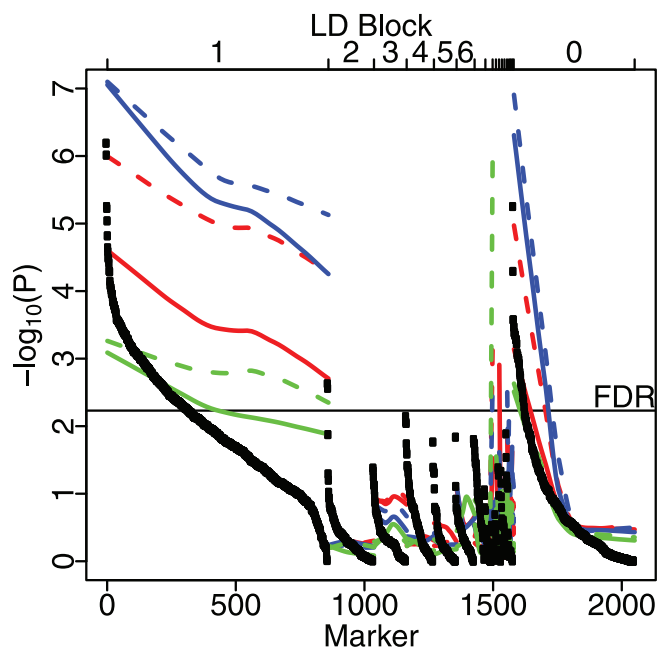


FIGURE 3 Overlap of DMR and phenylpropanoid marker associations. Black points = DMR-association $-\log_{10}(P)$ in descending strength from left to right for each linkage-disequilibrium (LD) block. Phenylpropanoid $-\log_{10}(P)$ -values are displayed as smoothed lines, blue line = n1121, red line = p3313, green line = n5122, continuous line = infected, dashed line = mock. The vertical line “FDR” corresponds to the highest p -value passing the false-discovery correction ($FDR < 0.05$, Benjamini and Hochberg, 1995)

coniferyl aldehyde/sinapyl alcohol (p3313, Tables S6 and S7). Only sinapoyl malate, cichoriin and esculin exhibited a significant overlap in the mock set (n4072; Figure 2, Table 2). Therefore, the statistical testing gave more evidence for a significant overlap of DMR and the production of phenylpropanoids at the same genetic loci.

3.11 | A DMR/phenylpropanoid regulatory candidate gene

Significant DMR associated markers formed 17 physical hotspots (Data S1) on four scaffolds. These hotspots, defined as the region spanned by the significant markers ± 50 kb, were BLAST-aligned. Seventy-eight unique homologous genes were found within all hotspots. Three protein kinase genes from a gene family related to pathogen resistance (Veronese et al., 2006) were found on hotspot 15 on scaffold 002101F (Table 3).

4 | DISCUSSION

4.1 | DMR is a metabolic phenomenon

We found a large proportion of metabolites (one out of three) to be induced upon infection, but it appears unlikely that all of these molecules would directly or indirectly contribute to resistance. Previous studies have shown that the level of phytohormones, such as jasmonic acid and salicylic acid, are elevated upon infection (Guerreiro, Figueiredo, Sousa Silva, & Figueiredo, 2016; Lakkis et al., 2019; Liu et al., 2016) and that these hormones may trigger signalling pathways, resulting in the production of specialized metabolites with a crucial role in DMR, such as phenylpropanoids, flavonols, stilbenes and stilbenoids (Batovska et al., 2009; Chitarrini et al., 2017). However, these studies often relied on measurements of a limited number of metabolites and may have overestimated the role of these metabolites within the entirety of the set of specialized metabolites present in an untargeted metabolomics dataset. The establishment of a systemic acquired resistance response with little effect on the pathogen may be a possible mechanism leading to the observed induction of specialized metabolites (Kulkarni et al., 2016). However, we found no indication of a protective activity of the induced specialized metabolites when comparing their variation with the resistance variation in our hop test population. It is plausible that hop does not possess an inducible and effective array of specialized metabolites against DM.

4.2 | DMR is largely prophylactic

A rather unexpected result of this study was the discovery that metabolite levels of uninfected plants are correlated with the degree of DMR of a replicate set of infected plants. In fact, the concordance and comparable degree of correlation between DMR-correlated metabolites from the infected and the mock datasets provides strong evidence that DMR

TABLE 2 Phenylpropanoids

ID	rt	R _{Infected}	R _{Mock}	χ^2_{Mock}	χ^2_{Infected}	Formula	KEGG structure	MS/MS scan ^a	MS/MS validation
p11841	10.6	-0.24	-0.20	0.1736	0.6627	C ₁₆ H ₁₈ O ₁₀	Fraxin	n.a.	No
n4563	21.5	-0.15	-0.28	0.42	0.2299	C ₁₆ H ₁₈ O ₉	Chlorogenic/Neochlorogenic acid ^b	1	Yes
p10896	22.6	-0.25	-0.23	NA	0.239	C ₁₆ H ₁₈ O ₉	Chlorogenic/Neochlorogenic acid ^b	2	Yes
n4566	42.1	-0.25	-0.26	0.3837	0.7938	C ₁₆ H ₁₈ O ₉	Chlorogenic/Neochlorogenic acid	n.a.	No
p10893	47.7	-0.27	-0.25	0.4204	0.6627	C ₁₆ H ₁₈ O ₉	Chlorogenic/Neochlorogenic acid ^c	3	Yes
n4564	48.1	-0.21	-0.27	0.4843	0.7938	C ₁₆ H ₁₈ O ₉	Chlorogenic/Neochlorogenic acid ^c	4	Yes
n3624	48.5	0.25	0.14	0.2123	NA	C ₁₅ H ₁₈ O ₈	cis-/trans-β-D-Glucosyl-2-hydroxycinnamic acid	5	No
n4500	52.0	-0.11	-0.23	0.7115	0.6627	C ₁₆ H ₁₈ O ₁₀	Fraxin	6	No
n5122	80.2	-0.17	-0.24	2.20E-16	9.36E-12	C ₁₆ H ₁₈ O ₁₀	Fraxin	n.a.	No
n1121	96.8	-0.20	-0.25	2.20E-16	2.20E-16	C ₉ H ₁₀ O ₂	4-Coumaryl alcohol	7	No
						C ₁₀ H ₁₂ O ₄	5-Hydroxyconiferyl alcohol	7	No
n4072	98.2	-0.09	-0.25	2.30E-07	0.3289	C ₁₅ H ₁₆ O ₉	Sinapoyl malate/Cichoriin/Esculin	8	No
p3313	109.3	-0.24	-0.20	4.25E-12	2.20E-16	C ₁₀ H ₁₀ O ₃	Coniferyl aldehyde	9	No
						C ₁₁ H ₁₄ O ₄	Sinapyl alcohol	9	No

Note: Correlation of phenylpropanoids extracted from either infected (R_{Infected}) or control (R_{Mock}) plants 48 hr after treatment to DMR in plants 7 days after infection (FDR < 0.1), and DMR overlap of association markers at DMR loci for both treatments mock (χ^2_{Mock}) and infected (χ^2_{Infected}).

Abbreviations: n, negative mode; n.a., no MS/MS spectrum recorded; p, positive mode.

^aScan No. in Data S2.

^{b,c}The putative chlorogenic/neochlorogenic acids eluting at ^brt = 21–23 s and ^crt = 47–49 s in both modes are likely identical.

TABLE 3 Candidate genes: Candidate genes in target organism *Arabidopsis thaliana* (Lamesch et al., 2012) on scaffold 002101F on the Cascade hop variety reference genome (Padgitt-Cobb et al., 2019) containing SNPs associated with DMR

Gene model	Gene description	Gene hit	Involved in	Query start	Query end	E-val	%ID
AT5G15080	Probable serine/threonine-protein kinase	PIX7	Defence response, protein phosphorylation	203862	204380	3E-70	73.7
AT2G39660	Botrytis-induced kinase	BIK1	Defence response to fungus, innate immune response, pattern recognition receptor signalling pathway, protein autophosphorylation	202060	202305	2E-42	61
AT3G09830	Pattern-triggered immunity kinase	PCRK1	Defence response to bacterium, pattern recognition receptor signalling pathway, protein phosphorylation, regulation of salicylic acid biosynthetic process,	203865	204164	9E-27	53

is established per se. Less than 1% of all specialized metabolites displayed significant correlations to resistance. The coefficients of correlation may appear low, but it has to be taken into account that (a) DMR was scored 5 days after sampling for metabolites, (b) DMR was scored visually and (c) DMR may not be conferred by the abundance of a single metabolite as is common in plant defence (innate or induced). These metabolites were typically not induced upon infection (Tables S1 and S2), again suggesting that resistance is not conferred by an inducible response but rather by the abundance of particular metabolites prior to a host-pathogen interaction. Such insufficient defence response has already been published in studies on grapevine that describe an inadequate up-regulation of genes encoding pathogenesis-related proteins or enzymes that are part of phenylpropanoid pathways once infected with

Plasmopara viticola (Ma et al., 2018; Nascimento et al., 2019). This presence of an insufficient defence mechanism in this species, in which the transient activation of defence genes and proteins is neither fast nor robust enough to prevent the spread of the pathogen, has been presented (Figueiredo et al., 2012, 2017; Kortekamp, 2006; Perazzoli et al., 2012; Polesani et al., 2010).

4.3 | Phenylpropanoids are key protective compounds

Phenylpropanoids show the strongest relative connection to DMR of the entirety of hundreds of annotated specialized metabolites

or thousands of unknown compounds with low polarity. The results provide evidence for an important metabolic DMR component regulated by the genetic control of phenylpropanoid levels. In a recent study, chlorogenic acid was shown to inhibit germination and growth as well as membrane permeabilization of pathogenic fungi (Martínez et al., 2017). In vitro studies with *p*-coumaric acid indicated that a concentration of 10 ppm was sufficient to inhibit the growth of *Phytium* sp. and *Corticium rolfsii* (Tawata et al., 1996). Others showed that coniferyl aldehyde may be a part of a mechanism for the restriction of *Melampsora lini* on flax leaves and may represent an effective phytoalexin for controlling fungal pathogens in the future (Keen & Littlefield, 1979). A number of studies (Bourgaud et al., 2006; Mabry & Ulubelen, 1980; Tiago et al., 2017) have shown that phenylpropanoid derivatives are able to protect plants against biotic infections by viruses, bacteria, or fungi. The resistance to the oomycete *Plasmopara viticola* in grapevine was found to coincide with stilbenoid accumulation, a subclass of phenylpropanoids (Figueiredo, Martins, Monteiro, Coelho, & Pais, 2015; Malacarne et al., 2011). The role of lignification and enzymes involved in the phenylpropanoid biosynthesis providing resistance has been investigated previously in other research (König et al., 2014; Langenbach, Campe, Schaffrath, Goellner, & Conrath, 2013; Matros & Mock, 2004). Monolignols are essential for cell wall reinforcement and are well known to play a role in the plant's defence response (Whetten & Sederoff, 1995).

Only *cis*-/*trans*- β -D-glucosyl-2-hydroxycinnamic acid was found to have a negative correlation with DMR in our study. Notably, this single positively correlated phenylpropanoid differs from the other negatively correlated ones by being glycosylated, and it is located in a different branch of the phenylpropanoid pathway than the candidates with a positive DMR function. Glycosylated phenylpropanoids are often accumulated in the vacuole and provide a reservoir or a protected form for the aglycons, that is, the biologically active non-glycosylated compounds (Roy, Huss, Creach, Hawkins, & Neutelings, 2016), suggesting that only the enzymatic conversion of this precursor to a phenylpropanoid will form an active compound. Furthermore, glycosylation in *A. thaliana* may play a role in maintaining a specific pool of pathogen-specific molecules in the phenylpropanoid pathway (Langenbach et al., 2013).

Testing of a cocktail of three phenylpropanoids showed that external application of these compounds indeed leads to a protection of the plants against infection with *P. humuli*. These putatively prophylactic compounds led to reduced leaf infection in 10 highly susceptible genotypes, thus validating their protective activity. Of course, we cannot estimate how much of the applied phenylpropanoids was incorporated into the leaf and if there was already a toxic effect on the pathogen on the leaf area, but transgenic plants with modified phenylpropanoid levels in biologically relevant amounts and distribution may validate their role in defence in the future. However, this finding not only supports the abovementioned notion that DMR occurs spontaneously in hop but also suggests that phenylpropanoid-mediated resistance against DM could be among the most powerful mechanisms inherent to hop against this disease.

At a metabolic level, changes in primary and secondary metabolism were also found to be related to *P. viticola* interactions, and few

metabolic markers for compatible and incompatible interactions were reported (Ali et al., 2009; Batovska et al., 2009; Buonassisi et al., 2017; Chitarrini et al., 2017).

4.4 | Major DMR locus likely confers resistance by regulating the phenylpropanoid biosynthetic pathway

We have thus applied a pseudo-testcross mapping strategy for the mapping of DMR and phenylpropanoid associated markers and only found major (on LG1) and smaller effect association (LG0) for both DMR and phenylpropanoids, indicating that the major contribution to resistance is mediated by these metabolites, in a heritable way. The putative protein kinases and phosphatases encoded within the scaffolds containing the associated markers could regulate the abundance of a number of phenylpropanoids by phosphorylation/dephosphorylation of regulators of expression of phenylpropanoid producing enzymes or such enzymes directly.

The understanding of genetic inheritance patterns in hop remains a major challenge and complicated the genetic analysis of DMR in this study. Significant deviation from Mendelian segregation expectations in diverse mapping populations has been repeatedly reported in the past (McAdam et al., 2013; Seefelder, Ehrmaier, Schweizer, & Seigner, 2000). The segregation phenomena in hop are similar to segregation distortion systems that are well described in other species known to exhibit chromosomal rearrangements (Carr & Carr, 1983; Golczyk, Massouh, & Greiner, 2014; Rauwolf, Golczyk, Meurer, Herrmann, & Greiner, 2008; Snow, 1960; Wiens & Barlow, 1975). Recent studies by Zhang et al. (2017) and Easterling et al. (2018) provide evidence that genomic regions are duplicated across the genome by translocation in hop. This translocation occurring in parents is differentially carried on into their progeny, so each offspring may have unique genomic structures, resulting in map discrepancies and mis-ordering of markers within linkage groups using recombination frequency as genetic distance between markers. Furthermore, recombination suppression leads to very strong linkage disequilibrium across the genome because large complete blocks of genome may be barred from participation in recombination due to pairing incompetence caused by translocation structures (Golczyk et al., 2014).

DMR in hops has been shown to be an inheritable and quantitative trait (Henning et al., 2015). Henning et al. investigated resistance to primary infection with downy mildew in hop, while our study focused on the secondary infection event. This might be the reason why different genetic markers and specialized metabolites associated with DMR were identified in the two studies. We found no significant co-incidence of DMR marker between the two datasets ($p = .5639$). Either the genes involved in these two events are different, or causative genes between the two rather different populations are different. This could be clarified by shifting the crossing partners between the populations.

The untargeted metabolite profiling and genome-wide association study contribute to a deeper understanding of the complex mechanisms of DMR in hop and provide substantial evidence for the

interdependences of specified metabolites and plant defence. These metabolic and genetic markers will increase breeding efficiency and create new opportunities for improvement of this valuable crop, reducing the amount of pesticides against DM.

ACKNOWLEDGMENTS

Annegret Laub and Dr. Lore Westphal (IPB) are gratefully acknowledged for their technical assistance during the inoculation experiments. We thank Andrea Apelt for excellent technical support in the LC-MS analyses. We are especially thankful to Harald Schwarz and Hopsteiner Senior Management for their help to realize this project. Funding for this study was provided by Simon H. Steiner, Hopfen, GmbH. Open access funding enabled and organized by Projekt DEAL.

CONFLICT OF INTEREST

No conflict of interest has been declared by the author(s).

AUTHOR CONTRIBUTIONS

Ludger A. Wessjohann, and Alexander Feiner: Initiated the work, **Ludger A. Wessjohann, Klaus Pillen, David Riewe, Paul Matthews and Alexander Feiner:** Created the workplan. **Alexander Feiner:** Performed the inoculation and phenotyping experiments. **David Riewe:** Measured polar metabolites in the F1 hop population. **David Riewe and Alexander Feiner:** Analysed all data. **Nicholi Pitra:** Processed GBS raw data and performed the variant calling. **Alexander Feiner and David Riewe:** Wrote the manuscript. **Paul Matthews, Ludger A. Wessjohann and Klaus Pillen:** Provided edits and supervision.

ORCID

Alexander Feiner  <https://orcid.org/0000-0001-6564-8826>

David Riewe  <https://orcid.org/0000-0002-9095-5518>

REFERENCES

- Ali, K., Maltese, F., Figueiredo, A., Rex, M., Fortes, A., Zyprian, E., ... Choi, Y. (2012). Alterations in grapevine leaf metabolism upon inoculation with *Plasmopara viticola* in different time-points. *Plant Science*, 191–192, 100–107. <https://doi.org/10.1016/j.plantsci.2012.04.014>
- Ali, K., Maltese, F., Zyprian, E., Rex, M., Choi, Y., & Verpoorte, R. (2009). NMR metabolic fingerprinting based identification of grapevine metabolites associated with downy mildew resistance. *Journal of Agricultural and Food Chemistry*, 57(20), 9599–9606. <https://doi.org/10.1021/jf902069f>
- Altschul, S., Gish, W., Miller, W., Myers, E., & Lipman, D. (1990). Basic local alignment search tool. *Journal of Molecular Biology*, 215(3), 403–410. [https://doi.org/10.1016/S0022-2836\(05\)80360-2](https://doi.org/10.1016/S0022-2836(05)80360-2)
- Batovska, D., Todorova, I., Parushev, S., Nedelcheva, D., Bankova, V., Popov, S., ... Batovski, S. (2009). Biomarkers for the prediction of the resistance and susceptibility of grapevine leaves to downy mildew. *Journal of Plant Physiology*, 166(7), 781–785. <https://doi.org/10.1016/j.jplph.2008.08.008>
- Becker, L., Poutaraud, A., Hamm, G., Muller, J., Merdinoglu, D., Carré, V., & Chaïmbault, P. (2013). Metabolic study of grapevine leaves infected by downy mildew using negative ion electrospray – Fourier transform ion cyclotron resonance mass spectrometry. *Analytica Chimica Acta*, 795, 44–51. <https://doi.org/10.1016/j.aca.2013.07.068>
- Benjamini, Y., & Hochberg, Y. (1995). Controlling the false discovery rate: A practical and powerful approach to multiple testing. *Journal of the Royal Statistical Society. Series B (Methodological)*, 57, 289–300. <https://doi.org/10.2307/2346101>
- Biendl, M., Enghard, B., Forster, A., Gahr, A., Lutz, A., Mitter, W., ... Schönberger, C. (2014). *Hops - their cultivation, composition and usage*. Nürnberg, Germany: Fachverlag Hans Carl GmbH.
- Bourgau, F., Hehn, A., Larbat, R., Doerper, S., Gontier, E., Kellner, S., & Matern, U. (2006). Biosynthesis of coumarins in plants: A major pathway still to be unravelled for cytochrome P450 enzymes. *Phytochemistry Reviews*, 5(2–3), 293–308. <https://doi.org/10.1007/s11101-006-9040-2>
- Box, G., & Cox, D. (1964). An analysis of transformations. *Journal of the Royal Statistical Society. Series B (Methodological)*, 26(2), 211–252.
- Bradbury, P., Zhang, Z., Kroon, D., Casstevens, T., Ramdoss, Y., & Buckler, E. (2007). TASSEL: Software for association mapping of complex traits in diverse samples. *Bioinformatics*, 23(19), 2633–2635. <https://doi.org/10.1093/bioinformatics/btm308>
- Broman, K., Wu, H., Sen, S., & Churchill, G. (2003). R/qtl: QTL mapping in experimental crosses. *Bioinformatics*, 19(7), 889–890. <https://doi.org/10.1093/bioinformatics/btg112>
- Bundessortenamt. (2000). *Richtlinien für die Durchführung von landwirtschaftlichen Wertprüfungen und Sortenversuchen*. Hannover, Germany: Landbuch Verlagsgesellschaft mbH. https://www.bundessortenamt.de/bsa/media/Files/Richtlinie_LW2000.pdf
- Buonassisi, D., Colombo, M., Migliaro, D., Dolzani, C., Peressotti, E., Mizzotti, C., ... Vezzulli, S. (2017). Breeding for grapevine downy mildew resistance: A review of 'omics' 'approaches'. *Euphytica*, 213(5), 103. <https://doi.org/10.1007/s10681-017-1882-8>
- Camañes, G., Scalschi, L., Vicedo, B., González-Bosch, C., & García-Agustín, P. (2015). An untargeted global metabolomic analysis reveals the biochemical changes underlying basal resistance and priming in *Solanum lycopersicum*, and identifies 1-methyltryptophan as a metabolite involved in plant responses to *Botrytis cinerea* and *Pseudomonas syringae*. *Plant Journal*, 84(1), 125–139. <https://doi.org/10.1111/tpj.12964>
- Carr, R., & Carr, G. (1983). Chromosome races and structural heterozygosity in *Calycadenia ciliosa* Greene (Asteraceae). *American Journal of Botany*, 70(5), 744–755. <https://doi.org/10.1002/j.1537-2197.1983.tb12454.x>
- Cerenak, A., Kralj, D., & Javornik, B. (2009). Compounds of essential oils as markers of hop resistance (*Humulus lupulus*) to powdery mildew (*Podosphaera macularis*). *Acta Agriculturae Slovenica*, 93(3), 267–273. <https://doi.org/10.2478/v10014-009-0015-z>
- Chitarrini, G., Soini, E., Riccadonna, S., Franceschi, P., Zulini, L., Masuero, D., ... Vrhovsek, U. (2017). Identification of biomarkers for defense response to *Plasmopara viticola* in a resistant grape variety. *Frontiers in Plant Science*, 8, 1–11. <https://doi.org/10.3389/fpls.2017.01524>
- Chong, J., Poutaraud, A., & Huguene, P. (2009). Metabolism and roles of stilbenes in plants. *Plant Science*, 177(3), 143–155. <https://doi.org/10.1016/j.plantsci.2009.05.012>
- Cleemput, M., Cattoor, K., Bosscher, K., Haegeman, G., Keukeleire, D., & Heyerick, A. (2009). Hop (*Humulus lupulus*)-derived bitter acids as multipotent bioactive compounds. *Journal of Natural Products*, 72, 1220–1230. <https://doi.org/10.3399/bjgp12X616418>
- Cohen, Y., & Eyal, H. (1980). Effects of light during infection on the incidence of downy mildew (*Pseudoperonospora cubensis*) on cucumbers. *Physiological Plant Pathology*, 17(1), 53–62.
- Darby, P. (2006). The history of hop breeding and development. *Journal of the Brewery History Society*, 121, 94–111.
- De Keukeleire, J., Ooms, G., Heyerick, A., Roldan-Ruiz, I., Van Bockstaele, E., & De Keukeleire, D. (2003). Formation and accumulation of α -acids, β -acids, desmethylxanthohumol, and xanthohumol during flowering of hops (*Humulus lupulus* L.). *Journal of Agricultural and Food Chemistry*, 51(15), 4436–4441. <https://doi.org/10.1021/jf034263z>

- Dixon, R. (2001). Natural products and plant disease resistance. *Nature*, 411(6839), 843–847. <https://doi.org/10.1038/35081178>
- Dixon, R., & Paiva, N. (1995). Stress-induced phenylpropanoid metabolism. *The Plant Cell*, 7(7), 1085–1097. <https://doi.org/10.1105/tpc.7.7.1085>
- Easterling, K., Pitra, N., Jones, R., Lopes, L., Aquino, J., Zhang, D., ... Bass, H. (2018). 3D molecular cytology of hop (*Humulus lupulus*) meiotic chromosomes reveals non-disomic pairing and segregation, aneuploidy, and genomic structural variation. *Frontiers in Plant Science*, 9, 1–13. <https://doi.org/10.3389/fpls.2018.01501>
- Farag, M., Mahrous, E., Lübken, T., Porzel, A., & Wessjohann, L. (2014). Classification of commercial cultivars of *Humulus lupulus* L. (hop) by chemometric pixel analysis of two dimensional nuclear magnetic resonance spectra. *Metabolomics*, 10(1), 21–32. <https://doi.org/10.1007/s11306-013-0547-4>
- Farag, M., Porzel, A., Schmidt, J., & Wessjohann, L. (2012). Metabolite profiling and fingerprinting of commercial cultivars of *Humulus lupulus* L. (hop): A comparison of MS and NMR methods in metabolomics. *Metabolomics*, 8(3), 492–507. <https://doi.org/10.1007/s11306-011-0335-y>
- Farag, M., Weigend, M., Luebert, F., Brokamp, G., & Wessjohann, L. (2013). Phytochemical, phylogenetic, and anti-inflammatory evaluation of 43 *Urtica* accessions (stinging nettle) based on UPLC-Q-TOF-MS metabolomic profiles. *Phytochemistry*, 96, 170–183. <https://doi.org/10.1016/j.phytochem.2013.09.016>
- Farag, M., & Wessjohann, L. (2013). Cytotoxic effect of commercial *Humulus lupulus* L. (hop) preparations - In comparison to its metabolomic fingerprint. *Journal of Advanced Research*, 4(4), 417–421. <https://doi.org/10.1016/j.jare.2012.07.006>
- Figueiredo, A., Martins, J., Monteiro, F., Coelho, A., & Pais, M. (2015). Early events of grapevine resistance towards downy mildew by a systems biology approach. *Revista de Ciências Agrárias*, 38(2), 124–130.
- Figueiredo, A., Martins, J., Sebastiana, M., Guerreiro, A., Silva, A., Matos, A., ... Coelho, A. (2017). Specific adjustments in grapevine leaf proteome discriminating resistant and susceptible grapevine genotypes to *Plasmopara viticola*. *Journal of Proteomics*, 152, 48–57. <https://doi.org/10.1016/j.jprot.2016.10.012>
- Figueiredo, A., Monteiro, F., Fortes, A., Bonow-Rex, M., Zyprian, E., Sousa, L., & Pais, M. (2012). Cultivar-specific kinetics of gene induction during downy mildew early infection in grapevine. *Functional & Integrative Genomics*, 12(2), 379–386. <https://doi.org/10.1007/s10142-012-0261-8>
- Gaspero, G., Cipriani, G., Adam-Blondon, A.-F., & Testolin, R. (2007). Linkage maps of grapevine displaying the chromosomal locations of 420 microsatellite markers and 82 markers for R-gene candidates. *Theoretical and Applied Genetics*, 114(7), 1249–1263. <https://doi.org/10.1007/s00122-007-0516-2>
- Gatica-Arias, A., Farag, M., Stanke, M., Matoušek, J., Wessjohann, L., & Weber, G. (2012). Flavonoid production in transgenic hop (*Humulus lupulus* L.) altered by PAP1/MYB75 from *Arabidopsis thaliana* L. *Plant Cell Reports*, 31(1), 111–119. <https://doi.org/10.1007/s00299-011-1144-5>
- Gent, D., Cohen, Y., & Runge, F. (2017). Homothallism in *Pseudoperonospora Humuli*. *Plant Pathology*, 66, 1508–1516. <https://doi.org/10.1111/ppa.12689>
- Golczyk, H., Massouh, A., & Greiner, S. (2014). Translocations of chromosome end-segments and facultative heterochromatin promote meiotic ring formation in evening primroses. *The Plant Cell*, 26(3), 1280–1293. <https://doi.org/10.1105/tpc.114.122655>
- Guerreiro, A., Figueiredo, J., Sousa Silva, M., & Figueiredo, A. (2016). Linking Jasmonic acid to grapevine resistance against the biotrophic oomycete *Plasmopara Viticola*. *Frontiers in Plant Science*, 7, 565. <https://doi.org/10.3389/fpls.2016.00565>
- Henning, J., Gent, D., Twomey, M., Townsend, M., Pitra, N., & Matthews, P. (2015). Precision QTL mapping of downy mildew resistance in hop (*Humulus lupulus* L.). *Euphytica*, 202(3), 487–498. <https://doi.org/10.1007/s10681-015-1356-9>
- Jiang, C., Sun, T., Xiang, D., Wei, S., & Li, W. (2018). Anticancer activity and mechanism of Xanthohumol: A prenylated flavonoid from hops (*Humulus lupulus* L.). *Frontiers in Pharmacology*, 9, 1–13. <https://doi.org/10.3389/fphar.2018.00530>
- Johnson, D., & Skotland, C. (1985). Effects of temperature and relative-humidity on sporangium production of *Pseudoperonospora-Humuli* on hop. *Phytopathology*, 75(2), 127–129.
- Kanehisa, M., & Goto, S. (2000). KEGG: Kyoto encyclopedia of genes and genomes. *Nucleic Acids Research*, 27(1), 29–34. <https://doi.org/10.1093/nar/27.1.29>
- Kavalier, A., Litt, A., Ma, C., Pitra, N., Coles, M., Kennelly, E., & Matthews, P. (2011). Phytochemical and morphological characterization of hop (*Humulus lupulus* L.) cones over five developmental stages using high performance liquid chromatography coupled to time-of-flight mass spectrometry, ultrahigh performance liquid chromatography photodiode array detection, and light microscopy techniques. *Journal of Agricultural and Food Chemistry*, 59(9), 4783–4793. <https://doi.org/10.1021/jf1049084>
- Keen, N., & Littlefield, L. (1979). The possible association of phytoalexins with resistance gene expression in flax to *Melampsora lini*. *Physiological Plant Pathology*, 14(3), 265–280. [https://doi.org/10.1016/0048-4059\(79\)90048-1](https://doi.org/10.1016/0048-4059(79)90048-1)
- König, S., Feussner, K., Kaever, A., Landesfeind, M., Thurow, C., Karlovsky, P., ... Feussner, I. (2014). Soluble phenylpropanoids are involved in the defense response of *Arabidopsis* against *Verticillium longisporum*. *The New Phytologist*, 202(3), 823–837. <https://doi.org/10.1111/nph.12709>
- Kortekamp, A. (2006). Expression analysis of defence-related genes in grapevine leaves after inoculation with a host and a non-host pathogen. *Plant Physiology and Biochemistry*, 44(1), 58–67. <https://doi.org/10.1016/j.plaphy.2006.01.008>
- Krajnovic, T., Draca, D., Kaluderovic, G., Dunderovic, D., Mirkov, I., Wessjohann, L., ... Mijatovic, S. (2019). The hop-derived prenylflavonoid Isoxanthohumol inhibits the formation of lung metastasis in B16-F10 murine melanoma model. *Food and Chemical Toxicology: An International Journal Published for the British Industrial Biological Research Association*, 129, 257–268. <https://doi.org/10.1016/j.fct.2019.04.046>
- Krajnovic, T., Kaluderovic, G., Wessjohann, L., Mijatovic, S., & Maksimovic-Ivanic, D. (2016). Versatile antitumor potential of Isoxanthohumol: Enhancement of paclitaxel activity in vivo. *Pharmacological Research*, 105, 62–73. <https://doi.org/10.1016/j.phrs.2016.01.011>
- Kuhl, C., Tautenhahn, R., Boettcher, C., Larson, T., & Neumann, S. (2012). CAMERA: An integrated strategy for compound spectra extraction and annotation of liquid chromatography/mass spectrometry data sets. *Analytical Chemistry*, 84, 283–289. <https://doi.org/10.1021/ac202450g>
- Kulkarni, K., Zala, H., Bosamia, T., Shukla, Y., Kumar, S., Fougat, R., ... Joshi, C. (2016). De novo transcriptome sequencing to dissect candidate genes associated with pearl millet-downy mildew (*Sclerospora graminicola* Sacc.) interaction. *Frontiers in Plant Science*, 7, 1–16. <https://doi.org/10.3389/fpls.2016.00847>
- Lakkis, S., Trotel-Aziz, P., Rabenoelina, F., Schwarzenberg, A., Nguema-Ona, E., Clément, C., & Aziz, A. (2019). Strengthening grapevine resistance by *Pseudomonas fluorescens* PTA-CT2 relies on distinct defense pathways in susceptible and partially resistant genotypes to downy mildew and gray Mold diseases. *Frontiers in Plant Science*, 10, 1–18. <https://doi.org/10.3389/fpls.2019.01112>
- Lamesch, P., Berardini, T., Li, D., Swarbreck, D., Wilks, C., Sasidharan, R., ... Huala, E. (2012). The *Arabidopsis* information resource (TAIR): Improved gene annotation and new tools. *Nucleic Acids Research*, 40(D1), 1202–1210. <https://doi.org/10.1093/nar/gkr1090>
- Langenbach, C., Campe, R., Schaffrath, U., Goellner, K., & Conrath, U. (2013). UDP-glucosyltransferase UGT84A2/BRT1 is required for *Arabidopsis* nonhost resistance to the Asian soybean rust pathogen

- Phakopsora pachyrhizi*. *The New Phytologist*, 198(2), 536–545. <https://doi.org/10.1111/nph.12155>
- Legay, G., Marouf, E., Berger, D., Neuhaus, J., Mauch-Mani, B., & Slaughter, A. (2011). Identification of genes expressed during the compatible interaction of grapevine with *Plasmopara viticola* through suppression subtractive hybridization (SSH). *European Journal of Plant Pathology*, 129(2), 281–301. <https://doi.org/10.1007/s10658-010-9676-z>
- Li, H., & Durbin, R. (2009). Fast and accurate short read alignment with burrows-wheeler transform. *Bioinformatics*, 25(14), 1754–1760. <https://doi.org/10.1093/bioinformatics/btp324>
- Li, H., Handsaker, B., Wysoker, A., Fennell, T., Ruan, J., Homer, N., ... Durbin, R. (2009). The sequence alignment/map format and SAMtools. *Bioinformatics*, 25(16), 2078–2079. <https://doi.org/10.1093/bioinformatics/btp352>
- Liu, S., Wu, J., Zhang, P., Hasi, G., Huang, Y., Lu, J., & Zhang, Y. (2016). Response of phytohormones and correlation of SAR signal pathway genes to the different resistance levels of grapevine against *Plasmopara viticola* infection. *Plant Physiology and Biochemistry*, 107, 56–66. <https://doi.org/10.1016/j.plaphy.2016.05.020>
- Ma, H., Xiang, G., Li, Z., Wang, Y., Dou, M., Su, L., ... Xu, Y. (2018). Grapevine VpPR10.1 functions in resistance to *Plasmopara viticola* through triggering a cell death-like defence response by interacting with VpVDAC3. *Plant Biotechnology Journal*, 16, 1488–1501. <https://doi.org/10.1111/pbi.12891>
- Mabry, T., & Ulubelen, A. (1980). Chemistry and utilization of phenylpropanoids including flavonoids, coumarins, and lignans. *Journal of Agricultural and Food Chemistry*, 28(2), 188–196. <https://doi.org/10.1021/jf60228a024>
- Maghuly, F., Pabinger, S., Krainer, J., & Laimer, M. (2018). The pattern and distribution of induced mutations in *J. curcas* using reduced representation sequencing. *Frontiers in Plant Science*, 9, 524. <https://doi.org/10.3389/fpls.2018.00524>
- Malacarne, G., Vrhovsek, U., Zulini, L., Cestaro, A., Stefanini, M., Mattivi, F., ... Moser, C. (2011). Resistance to *Plasmopara viticola* in a grapevine segregating population is associated with stilbenoid accumulation and with specific host transcriptional responses. *BMC Plant Biology*, 11(1), 114. <https://doi.org/10.1186/1471-2229-11-114>
- Martínez, G., Regente, M., Jacobi, S., Del Rio, M., Pinedo, M., & de la Canal, L. (2017). Chlorogenic acid is a fungicide active against phytopathogenic fungi. *Pesticide Biochemistry and Physiology*, 140, 30–35. <https://doi.org/10.1016/j.pestbp.2017.05.012>
- Matros, A., & Mock, H. (2004). Ectopic expression of a UDP-glucose: Phenylpropanoid glucosyltransferase leads to increased resistance of transgenic tobacco plants against infection with Potato Virus Y. *Plant & Cell Physiology*, 45(9), 1185–1193. <https://doi.org/10.1093/pcp/pch140>
- McAdam, E., Freeman, J., Whittock, S., Buck, E., Jakse, J., Cerenak, A., ... Koutoulis, A. (2013). Quantitative trait loci in hop (*Humulus lupulus* L.) reveal complex genetic architecture underlying variation in sex, yield and cone chemistry. *BMC Genomics*, 14, 360. <https://doi.org/10.1186/1471-2164-14-360>
- Milli, A., Ceconi, D., Bortesi, L., Persi, A., Rinalducci, S., Zamboni, A., ... Polverari, A. (2012). Proteomic analysis of the compatible interaction between *Vitis vinifera* and *Plasmopara viticola*. *Journal of Proteomics*, 75(4), 1284–1302. <https://doi.org/10.1016/j.jprot.2011.11.006>
- Miranda, C., Johnson, L., De Montgolfier, O., Elias, V., Ullrich, L., Hay, J., ... Stevens, J. F. (2018). Non-estrogenic Xanthohumol derivatives mitigate insulin resistance and cognitive impairment in high-fat diet-induced obese mice. *Scientific Reports*, 8(1), 1–17. <https://doi.org/10.1038/s41598-017-18992-6>
- Mitchell, M., Ocamb, C., Grunwald, N., Mancino, L., & Gent, D. (2011). Genetic and pathogenic relatedness of *Pseudoperonospora cubensis* and *P. Humuli*. *Phytopathology*, 101(7), 805–818. <https://doi.org/10.1094/PHYTO-10-10-0270>
- Nascimento, R., Maia, M., Ferreira, A., Silva, A., Freire, A., Cordeiro, C., ... Figueiredo, A. (2019). Early stage metabolic events associated with the establishment of *Vitis vinifera* – *Plasmopara viticola* compatible interaction. *Plant Physiology and Biochemistry*, 137, 1–13. <https://doi.org/10.1016/j.plaphy.2019.01.026>
- NCBI. (2018). *National Center for Biotechnology Information*.
- Negrel, L., Halter, D., Wiedemann-Merdinoglu, S., Rustenholz, C., Merdinoglu, D., Huguene, P., & Baltenweck, R. (2018). Identification of lipid markers of *Plasmopara viticola* infection in grapevine using a non-targeted metabolomic approach. *Frontiers in Plant Science*, 9, 1–11. <https://doi.org/10.3389/fpls.2018.00360>
- Neve, R. (1991). *Hops*. Dordrecht, the Netherlands: Springer. Retrieved from <http://doi.org/10.1007/978-94-011-3106-3>
- Padgitt-Cobb, L., Kingan, S., Wells, J., Elser, J., Kronmiller, B., Moore, D., ... Hendrix, D. A. (2019). A phased, diploid assembly of the Cascade hop (*Humulus lupulus*) genome reveals patterns of selection and haplotype variation. *BioRxiv*. Retrieved from <https://doi.org/10.1101/786145>.
- Perazzolli, M., Moretto, M., Fontana, P., Ferrarini, A., Velasco, R., Moser, C., ... Pertot, I. (2012). Downy mildew resistance induced by *Trichoderma harzianum* T39 in susceptible grapevines partially mimics transcriptional changes of resistant genotypes. *BMC Genomics*, 13(1), 1–19. <https://doi.org/10.1186/1471-2164-13-660>
- Polesani, M., Bortesi, L., Ferrarini, A., Zamboni, A., Fasoli, M., Zadra, C., ... Polverari, A. (2010). General and species-specific transcriptional responses to downy mildew infection in a susceptible (*Vitis vinifera*) and a resistant (*V. riparia*) grapevine species. *BMC Genomics*, 11, 117. <https://doi.org/10.1186/1471-2164-11-117>
- Polesani, M., Desario, F., Ferrarini, A., Zamboni, A., Pezzotti, M., Kortekamp, A., & Polverari, A. (2008). CDNA-AFLP analysis of plant and pathogen genes expressed in grapevine infected with *Plasmopara viticola*. *BMC Genomics*, 9, 1–14. <https://doi.org/10.1186/1471-2164-9-142>
- Possemmer, S., Bolca, S., Grootaert, C., Heyerick, A., Decroos, K., Dhooze, W., ... Van de Wiele, T. (2006). The Prenylflavonoid Isoxanthohumol from hops (*Humulus lupulus* L.) is activated into the potent phytoestrogen 8-prenylnaringenin in vitro and in the human intestine. *The Journal of Nutrition*, 136(7), 1862–1867. <https://doi.org/10.1093/jn/136.7.1862>
- R Development Core Team. (2018). *R: A language and environment for statistical computing*. Vienna, Austria: R Foundation for Statistical Computing. Retrieved from <http://www.r-project.org/>
- Rauwolf, U., Golczyk, H., Meurer, J., Herrmann, R., & Greiner, S. (2008). Molecular marker systems for *Oenothera* genetics. *Genetics*, 180(3), 1289–1306. <https://doi.org/10.1534/genetics.108.091249>
- Riewe, D., Jeon, H., Lisec, J., Heuermann, M., Schmeichel, J., Seyfarth, M., ... Altmann, T. (2016). A naturally occurring promoter polymorphism of the Arabidopsis FUM2 gene causes expression variation, and is associated with metabolic and growth traits. *Plant Journal*, 88(5), 826–838. <https://doi.org/10.1111/tpj.13303>
- Riewe, D., Koohi, M., Lisec, J., Pfeiffer, M., Lippmann, R., Schmeichel, J., ... Altmann, T. (2012). A tyrosine aminotransferase involved in tocopherol synthesis in Arabidopsis. *Plant Journal*, 71(5), 850–859. <https://doi.org/10.1111/j.1365-3113X.2012.05035.x>
- Riewe, D., Wiebach, J., & Altmann, T. (2017). Structure annotation and quantification of wheat seed oxidized lipids by high resolution LC-MS/MS. *Plant Physiology*, 175, 600–618. <https://doi.org/10.1104/pp.17.00470>
- Rossbauer, G. (1995). BBCH-Codierung Der Phänologischen Entwicklungsstadien von Hopfen (*Humulus lupulus* L.). Landesanstalt für Landwirtschaft, Hopfen.
- Roy, J., Huss, B., Creach, A., Hawkins, S., & Neutelings, G. (2016). Glycosylation is a major regulator of phenylpropanoid availability and biological activity in plants. *Frontiers in Plant Science*, 7(735), 1–19. <https://doi.org/10.3389/fpls.2016.00735>

- Royle, D., & Thomas, G. (1971). The influence of stomatal opening on the infection of hop leaves by *Pseudoperonospora humuli*. *Physiological Plant Pathology*, 1(3), 329–343. [https://doi.org/10.1016/0048-4059\(71\)90053-1](https://doi.org/10.1016/0048-4059(71)90053-1)
- Royle, D., & Thomas, G. (1973). Factors affecting zoospore responses towards stomata in hop downy mildew (*Pseudoperonospora humuli*) including some comparisons with grapevine downy mildew (*Plasmopara viticola*). *Physiological Plant Pathology*, 3(3), 405–417. [https://doi.org/10.1016/0048-4059\(73\)90013-1](https://doi.org/10.1016/0048-4059(73)90013-1)
- Seefeldt, S., Ehrmaier, H., Schweizer, G., & Seigner, E. (2000). Male and female genetic linkage map of hops, *Humulus lupulus*. *Plant Breeding*, 119, 249–255.
- Smith, C., Want, E., O'Maille, G., Abagyan, R., & Siuzdak, G. (2006). XCMS: Processing mass spectrometry data for metabolite profiling using nonlinear peak alignment, matching, and identification. *Analytical Chemistry*, 78(3), 779–787. <https://doi.org/10.1021/ac051437y>
- Snow, R. (1960). Chromosomal differentiation in *Clarkia dudleyana*. *American Journal of Botany*, 47(4), 302–309. <https://doi.org/10.1002/j.1537-2197.1960.tb07129.x>
- Stevens, J., & Page, J. (2004). Xanthohumol and related prenylflavonoids from hops and beer: To your good health! *Phytochemistry*, 65(10), 1317–1330. <https://doi.org/10.1016/j.phytochem.2004.04.025>
- Su, H., Jiao, Y., Wang, F., Liu, Y., Niu, W., Liu, G., & Xu, Y. (2018). Over-expression of VpPR10.1 by an efficient transformation method enhances downy mildew resistance in *V. vinifera*. *Plant Cell Reports*, 37(5), 819–832. <https://doi.org/10.1007/s00299-018-2271-z>
- Tawata, S., Taira, S., Kobamoto, N., Zhu, J., Ishihara, M., & Toyama, S. (1996). Synthesis and antifungal activity of cinnamic acid esters. *Bioscience, Biotechnology, and Biochemistry*, 60(5), 909–910.
- Tenenbaum, D. (2018). KEGGREST: Client-side REST access to KEGG. R Package Version 1.20.0.
- Thiele, H., Mcleod, G., Niemitz, M., & Kühn, T. (2011). Structure verification of small molecules using mass spectrometry and NMR spectroscopy. *Monatshefte Für Chemie - Chemical Monthly*, 142, 717–730. <https://doi.org/10.1007/s00706-011-0486-6>
- Tiago, O., Maicon, N., Ivan, R., Diego, N., Vinicius, J., Mauricio, F., ... Velci, Q. (2017). Plant secondary metabolites and its dynamical systems of induction in response to environmental factors: A review. *African Journal of Agricultural Research*, 12(2), 71–84. <https://doi.org/10.5897/AJAR2016.11677>
- Toffolatti, S., Venturini, G., Maffi, D., & Vercesi, A. (2012). Phenotypic and histochemical traits of the interaction between *Plasmopara viticola* and resistant or susceptible grapevine varieties. *BMC Plant Biology*, 12(1), 1. <https://doi.org/10.1186/1471-2229-12-124>
- USDA. (2018). *USDA natural resources conservation service*. Retrieved from <https://plants.usda.gov/core/profile?symbol=hulu>
- Vannozzi, A., Dry, I., Fasoli, M., Zenoni, S., & Lucchin, M. (2012). Genome-wide analysis of the grapevine stilbene synthase multigenic family: Genomic organization and expression profiles upon biotic and abiotic stresses. *BMC Plant Biology*, 12, 130. <https://doi.org/10.1186/1471-2229-12-130>
- Van Ooijen, J. (2011). Multipoint maximum likelihood mapping in a full-sib family of an outbreeding species. *Genetics Research*, 93(5), 343–349. <https://doi.org/10.1017/S0016672311000279>
- Veronese, P., Nakagami, H., Bluhm, B., Abuqamar, S., Chen, X., Salmeron, J., ... Mengiste, T. (2006). The membrane-anchored BOTRYTIS-INDUCED KINASE1 plays distinct roles in Arabidopsis resistance to necrotrophic and biotrophic pathogens. *The Plant Cell*, 18(1), 257–273. <https://doi.org/10.1105/tpc.105.035576>
- Vogt, T. (2010). Phenylpropanoid biosynthesis. *Molecular Plant*, 3(1), 2–20. <https://doi.org/10.1093/mp/ssp106>
- Wang, Y., Chantreau, M., Sibout, R., & Hawkins, S. (2013). Plant cell wall lignification and monolignol metabolism. *Frontiers in Plant Science*, 4, 1–14. <https://doi.org/10.3389/fpls.2013.00220>
- Weidenbach, D., Jansen, M., Franke, R., Hensel, G., Weissgerber, W., Ulferts, S., ... Schaffrath, U. (2014). Evolutionary conserved function of barley and Arabidopsis 3-KETOACYL-CoA SYNTHASES in providing wax signals for germination of powdery mildew fungi. *Plant Physiology*, 166(3), 1621–1633. <https://doi.org/10.1104/pp.114.246348>
- Whetten, R., & Sederoff, R. (1995). Lignin biosynthesis. *The Plant Cell*, 7(7), 1001–1013. <https://doi.org/10.1105/tpc.7.7.1001>
- Wiebach, J., Nagel, M., Borner, A., Altmann, T., & Riewe, D. (2019). Age-dependent loss of seed viability is associated with increased lipid oxidation and hydrolysis. *Plant, Cell & Environment*, 43, 303–314. <https://doi.org/10.1111/pce.13651>
- Wiens, D., & Barlow, B. (1975). Permanent translocation heterozygosity and sex determination in East African mistletoes. *Science*, 187(4182), 1208–1209. <https://doi.org/10.1126/science.187.4182.1208>
- Wilhelm, H., & Wessjohann, L. (2006). An efficient synthesis of the phytoestrogen 8-prenylnaringenin from xanthohumol by a novel demethylation process. *Tetrahedron*, 62(29), 6961–6966. <https://doi.org/10.1016/j.tet.2006.04.060>
- Xin, Z., & Chen, J. (2012). A high throughput DNA extraction method with high yield and quality. *Plant Methods*, 8(1), 26. <https://doi.org/10.1186/1746-4811-8-26>
- Zhang, D., Easterling, K., Pitra, N., Coles, M., Buckler, E., Bass, H., & Matthews, P. (2017). Non-Mendelian single-nucleotide polymorphism inheritance and atypical meiotic configurations are prevalent in hop. *The Plant Genome*, 10(3), 1–14. <https://doi.org/10.3835/plantgenome2017.04.0032>

SUPPORTING INFORMATION

Additional supporting information may be found online in the Supporting Information section at the end of this article.

How to cite this article: Feiner A, Pitra N, Matthews P, Pillen K, Wessjohann LA, Riewe D. Downy mildew resistance is genetically mediated by prophylactic production of phenylpropanoids in hop. *Plant Cell Environ*. 2021;44: 323–338. <https://doi.org/10.1111/pce.13906>